Calculation of the electronic structure and related physical properties of platinum*

F. Y. Fradin and D. D. Koelling
Argonne National Laboratory, Argonne, Illinois 60439

A. J. Freeman and T. J. Watson-Yang
Physics Department, Northwestern University, Evanston, Illinois 60201

(Received 22 May 1975)

The electronic band structure, density of states, and Fermi surface of Pt metal have been calculated using the relativistic-augmented-plane-wave method. The Fourier series representation of the *a priori* band structure has been found to yield a Fermi surface in good agreement with the de Haas–van Alphen results. The subband densities of states of platinum have been calculated with 0.25-mRy resolution using a tetrahedron scheme. The temperature dependences of the spin susceptibility, the electrical resistivity, the nuclear spin-lattice relaxation rate, and the electronic-specific-heat coefficient have been calculated in the constant-matrix-element approximation and have been found to be in reasonable agreement with the experimental results.

I. INTRODUCTION

Interest in Pd and Pt metals and their alloys remains high because of their remarkable and as yet not well-understood electric and magnetic properties. Their large exchange-enhancement parameters[1] make them ideal candidates for observing paramagnons, or persistent spin fluctuations, which were first postulated to explain the absence of superconductivity at the end of the transition-metal series.[2] Their low-temperature resistivity follows a T^2 law, a behavior which has been described in terms of spin fluctuations.

Recently, mounting evidence has led to a critical review[3] of the proposed existence of paramagnons in metals and to the conclusion that their existence, in fact, has not been established for the nearly ferromagnetic metallic systems like Pd and Pt. Very recently, the sharp structure found in the *ab initio* calculations[4,5] of the density of states in Pd metal has led to theoretical calculations of the temperature dependence of the resistivity[6] (and also the spin susceptibility[7,6]) that are in very good agreement with experiment above 20 K. These results were obtained entirely without invoking spin-fluctuation contributions.

Interest in Pt metal is high because of its close relationship to its sister metal Pd. Many of their electronic properties are very similar, as expected from their similar band structure and Fermi surface. A notable difference is the smaller value of the exchange-enhancement factor found for Pt (~4) compared with that of Pd (~8). We have studied the temperature dependence of a number of properties of Pt in order to confirm the above-mentioned results for Pd and to investigate possible differences arising from the greater importance of relativistic effects (notably spin-orbit splitting) on the band structure of Pt metal. In this paper, we determine the temperature dependence of the resistivity, the magnetic susceptibility, the electronic specific heat, and the spin-lattice relaxation time due to effects of sharp structure in the electronic density of states as found from a relativistic-augmented-plane-wave (RAPW) calculation. The results are found to be in good agreement with experiment and confirm the important role played by structure in the density of states.

II. THEORETICAL DETERMINATION OF BAND STRUCTURE, FERMI SURFACE, AND DENSITY OF STATES

The electronic structure of Pd and Pt metals has been studied extensively both experimentally[8,9] and theoretically.[4,5] The electronic band structure, Fermi surface, and density of states of Pt metal have been determined previously by Anderson and collaborators.[5] For Pt they used a muffin-tin approximation to the potential derived from the overlap of atomic Dirac-Fock charge densities calculated from the atomic configuration $5d^9 6s^1$. Detailed comparison with the Fermi-surface dimensions obtained from the de Haas–van Alphen data of Ketterson *et al.*[8,9] showed the agreement to be very good. The shape of the Fermi surfaces of Pd and Pt are found to be remarkably similar. Each metal has a closed electron surface centered about Γ (the center of the Brillouin zone), a small-volume closed-hole surface centered about X and a large-volume open-hole surface (the "jungle gym") also centered about the X point. The good agreement between theory and experiment has given a large measure of confidence to the validity of the band calculations.

For our calculations, the energy eigenvalues $\epsilon_n(k)$ were obtained using the relativistic-augmented-plane-wave (RAPW) method[10] applied to a warped-muffin-tin (WMT) approximation[11] to

the crystal potential. The crystal potential was constructed from the standard overlapping atomic charge density model using the Slater ($\alpha = 1$) exchange approximation.[12] The Pt atomic charge density used in the overlapping procedure was calculated using a Dirac-Slater code[13] for an assumed $5d^{10}6s^0$ configuration as this corresponds more closely to the almost full d-band structure of the metal. The radial mesh was adjusted so that the 321st mesh point occurred at the radius of touching muffin-tin spheres for the lattice constant used ($a = 7.3983$ a.u. vs 7.4137 of Andersen *et al.*[5]). In this manner, it was possible to maximize the volume of the muffin-tin spheres used while maintaining the convenience of having the radius of the muffin-tin sphere fall at a mesh point. With the exception of the different atomic configuration for the Dirac-Slater atomic charge density calculations, radial mesh, and muffin-tin radius, the crystal potential model is the same as that used previously.[5]

RAPW energy eigenvalues were obtained on a cubic mesh of linear dimension ($\pi/6a$) within $\frac{1}{48}$ of the Brillouin zone (BZ). These eigenvalues were then least-squares fit with a Fourier series that included 60 stars of primitive translation vectors. (The wave vectors used in a Fourier series of a quantity such as the energy-band structure, with Γ_1 symmetry in reciprocal space, are the primitive translation vectors of the real space.) The quality of the fits to the first six bands is good; the rms error is about 2 mRy for the first five bands and twice this value for the 6th band; the maximum differences between the RAPW and the fitted eigenvalues is about two times the rms errors quoted. All further calculated results to be presented here were performed using the Fourier-series representation of the bands.

The density of states was calculated by subdividing the irreducible $\frac{1}{48}$ of the BZ into 6144 tetrahedrons within which the dispersion relation was assumed to be linear. The density of states is then given by a sum on analytic expressions for each tetrahedron.[14] The resultant total density of states near the Fermi energy ($E_F = 0.6215$ Ry) is shown in Fig. 1 along with its band by band decomposition. The contribution of band 4 is not shown as it is too small to be plotted on this scale. As can be seen, all the structure near the Fermi energy arises from band 5 since band 6 has a very nearly constant density of states in this energy region.

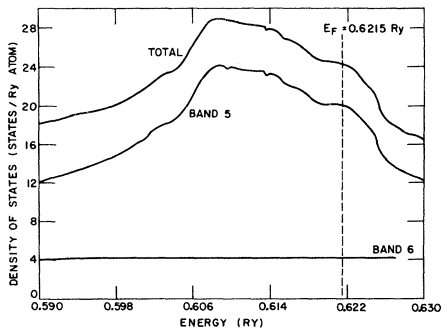

FIG. 1. Density of states of Pt: energy-scale resolution equals 0.25 mRy; $E_F = 0.6215$ Ry.

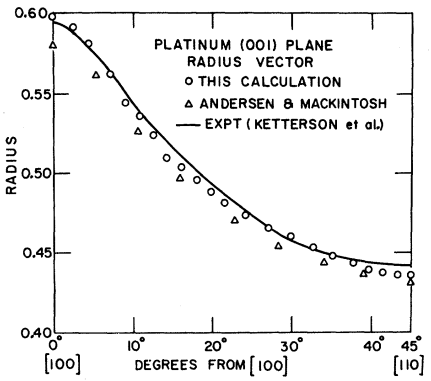

FIG. 2. Radius vector of Γ centered piece of the Fermi surface of Pt in the (001) plane: the solid line denotes the experimental data (Ref. 8); the triangles denote the theoretical values of Andersen and Mackintosh (Ref. 5).

Given the Fermi energy and a convenient representation (Fourier series) for the band structure, it is a simple matter to construct and check the Fermi surface. This has been done and we find very good agreement with the experimental data[9] and with the previous calculation of Anderson and Mackintosh.[5] As an example, we show in Fig. 2 the Fermi radius plot for the Γ centered piece in the (100) plane. We see that our results are in somewhat better agreement with the experimental results than are the values of Anderson and Mackintosh. What is rather surprising is the very close agreement obtained for all our results with those of Anderson and Mackintosh in view of the different potentials used in the two sets of calculations. Particularly noteworthy, is the insensitivity of the results to warping and to the use of different configurations for the atomic charge densities.

III. TEMPERATURE DEPENDENCE OF PHYSICAL PROPERTIES

In this section the temperature dependences of a number of physical properties are calculated. The energy-space representation is used. That is, we calculate integrals over $N(\epsilon)$ and $f(\epsilon, \mu, T)$, where f is the Fermi-Dirac distribution. This procedure is only appropriate above about 20 K, where the momentum selection rules should be relatively unimportant, i.e., the scattering of electrons by phonons yields values of Δk of order

k_F. We, however, use a rigid $N(\epsilon)$ so that we are not taking into account thermal expansion of the lattice. This will be an increasing source of error as T increases beyond $\theta_D \approx 230$ K. Because of the structure in $N(\epsilon)$, we have calculated $\mu(T)$ by iteration so that the number of occupied states is held constant to within five parts in 10^7.

A. Electronic heat capacity

The temperature dependence of the bare electronic-specific-heat coefficient γ_0 normalized by the $T=0$ K value is shown in Fig. 3. The change of $\gamma_0(T)$ of -30% at 700 K is somewhat smaller than that used by Knapp and Jones[15] in the extrapolation of the high-temperature experimental γ_0 value to $T=0$. Also shown in Fig. 3 is the shift $\mu(T)-\mu(0)$ in the chemical potential with temperature. Although $\mu(T)$ is roughly parabolic, deviations from parabolic behavior above 100 K are apparent in $\gamma_0(T)$. The calculated value of $\gamma_0(T=0)=24.29$ Ry^{-1} or 1.786 eV^{-1} can be combined with the experimental enhanced electronic-specific-heat coefficient $\gamma(T=0)=\gamma_0(T=0)(1+\lambda)$ of 2.83 eV^{-1} to yield a value of $\lambda=0.59$, in good agreement with the ratio of low-to-high-temperature γ values.[15] Since $\gamma(T>\theta_D)=\gamma_0(T)$, the ratio yields[15] $\lambda=0.6\pm0.1$.

B. Magnetic susceptibility

The analysis of Knight shift and susceptibility of Pt by Clogston *et al.*[16] shows that the sum of the van Vleck second-order orbital susceptibility, Pauli spin susceptibility of the s band, and the diagmagnetic susceptibility approximately sum to zero. Thus, the measured susceptibility should be equal to the Pauli susceptibility of the d band. We use the molecular field treatment of exchange enhancement for the susceptibility

$$\chi=\chi_0\,(1-I\chi_0)^{-1}\ , \tag{1}$$

where χ_0 is the unenhanced susceptibility and I is treated as a temperature-independent exchange constant. $\chi_0(T)$ is calculated from

$$\chi_0(T)=\frac{2\mu_B^2}{k_BT}\int N(\epsilon)\,f(\epsilon)\,[1-f(\epsilon)]\,d\epsilon\ , \tag{2}$$

where μ_B is the Bohr magneton and k_B is Boltzmann's constant. In Fig. 4 we plot $\chi^{-1}=\chi_0^{-1}-I$. The theoretical calculation of χ^{-1} is quite sensitive to the exact placement of $E_F=\mu(0)$. Movement of E_F by as little as 100 K makes significant changes in χ^{-1}. However, a consistent feature of the experimental results and the theoretical calculations is the shoulder in χ^{-1} near 120 K. The theoretical curve shown is for $E_F=98079$ K (0.621 Ry). The theoretical curve was forced to fit experiment at 100 K by adjusting the Stoner factor $\alpha=I\chi_0(0)=0.724$. This results in a $T=0$ exchange enhancement of $S(0)=(1-\alpha)^{-1}=3.62$. We note that the upturn in the experimental susceptibility[17] below about 20 K is undoubtedly associated with magnetic impurities.

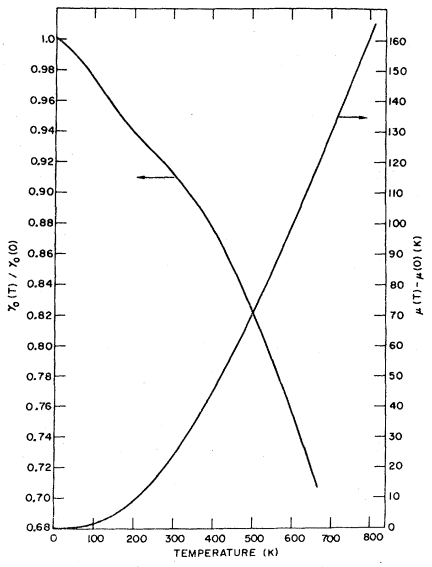

FIG. 3. Calculated temperature dependence of the electronic-specific-heat coefficient γ_0 normalized to the $T=0$ value and calculated shift of the chemical potential $\mu(T)-\mu(0)$ with temperature.

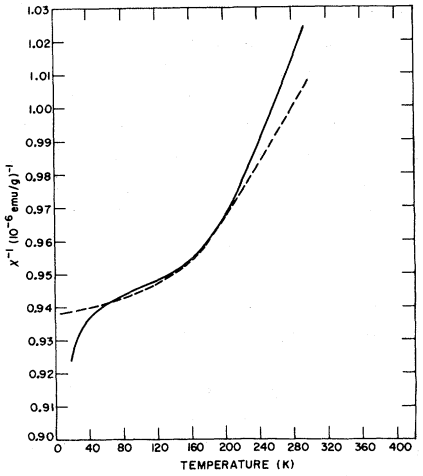

FIG. 4. Inverse magnetic susceptibility of Pt: solid curve, experimental data of Budworth *et al.* (Ref. 17); dashed curve, calculated value with $(1-\alpha)^{-1}=3.62$.

C. Electrical resistivity

In Fig. 5 we plot the electrical resistivity of Pt and of Au. The electrical resistivity of a transition metal has two major contributions; the intraband scattering of the light mass s electrons by the phonons $\rho_{s\text{-}s}$ and the interband scattering of the s electrons into d states near E_F by

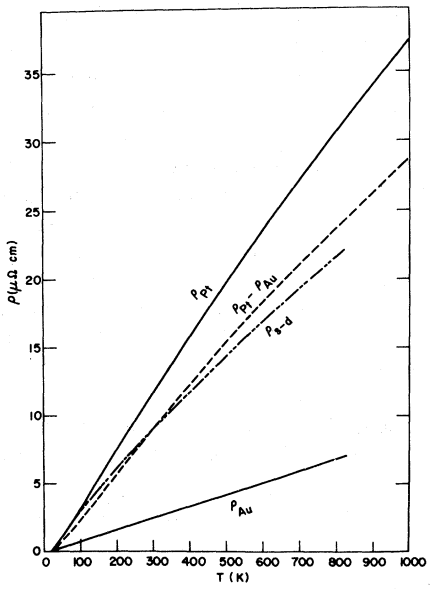

FIG. 5. Electrical resistivity of Pt and Au. The calculated value of ρ_{s-d} has been adjusted to be equal to $\rho_{Pt}-\rho_{Au}$ at 280 K.

the phonons ρ_{s-d}. As shown by Fradin[6] for Pd, the latter term ρ_{s-d} can have significant deviations from the classical linear T dependence at high temperatures due to structure in $N(\epsilon)$ near E_F. We estimate the contribution ρ_{s-s} in Pt as equal to the resistivity of Au. The difference $\rho_{Pt}-\rho_{Au}$ is then compared to the calculated term ρ_{s-d}. Here ρ_{s-d} is calculated from the expression for phonon absorption

$$\rho_{s-d}=\frac{\rho_0}{k_B T}\int_0^{\theta_D}\frac{3\omega^2 d\omega}{\theta_D^3}n(\omega)\int d\epsilon\,\frac{N_d(\epsilon+\omega)}{N(0)}$$

$$\times f(\epsilon)\,[1-f(\epsilon+\omega)]\ , \qquad (3)$$

where ρ_0 is a constant, $n(\omega)$ is the Bose function, and $N_d(\epsilon)$ is the d fraction of the total density of states (assumed to be equivalent to the 5th band density of states of Fig. 1). To calculate the contribution to ρ_{s-d} from phonon emission, $n(\omega)$ is replaced by $n(\omega)+1$ and $\epsilon+\omega$ goes over to $\epsilon-\omega$. We note that ρ_{s-d} is not nearly as sensitive as χ, with regards to the placement of E_F, owing to the additional integral over the phonon states, assumed Debye-like. Because of the difficulty of estimating umklapp contributions ρ_0 is left as a free parameter that has been fixed by setting $\rho_{s-d}=\rho_{Pt}-\rho_{Au}$ at 280 K. Although there is only modest agreement, both experiment and theory have a similar concave downwards appearance. In the calculation of ρ_{s-d}, no attempt has been made to adjust the Debye spectrum to account for anharmonicity due to thermal expansion, etc.

D. Nuclear spin-lattice relaxation rate

The nuclear spin-lattice relaxation rate of ^{195}Pt, T_1^{-1}, has been measured between 20 and 290 K by Butterworth.[18] The experimental values of $(T_1T)^{-1}$ normalized by the 20-K value are shown in Fig. 6. Yafet and Jaccarino[19] have discussed the various contributions to T_1^{-1} at $T=0$ K. However, their estimates were based on the electronic-specific-heat coefficient measured at low temperature $\gamma(T\simeq 0)$. They did not correct for the electron mass enhancement[15] λ, i.e., $\gamma(0)=\gamma_0(0)\,(1+\lambda)$. If we correct their estimates of the contribution to T_1^{-1} from the d-spin core polarization interaction and from the d-orbtial hyperfine interaction by $(1+\lambda)^{-2}$ and if we take account of the exchange enhancement of the d-spin core polarization contribution $\sim\kappa(\alpha)\,S^2(0)=0.52\times 13.1=6.8$ for $\alpha=0.72$, we find that the temperature-dependent core-polarization contribution is approximately 50% of the total relaxation rate at $T=0$ K. Here $\kappa(\alpha,T)$ represents the reduction of exchange effects on T_1^{-1} due to the q dependence of $\chi_0(q,0,T)$.[20]

Jullien and Coqblin[21] have shown for a parabolic electron energy dispersion that $\kappa(\alpha,T)=[(1/T_1T)/(1/T_1T)_{\alpha=0}]\,[2\mu_B^2N(0)/\chi(0,0,T)]^2$ is independent of α. That is $\kappa(\alpha,T)$ can be represented as $\kappa(\alpha,T)=C(\alpha)\kappa(0,T)$ for all α, where C is a temperature-independent constant. Assuming this result is more general, we write the core polarization con-

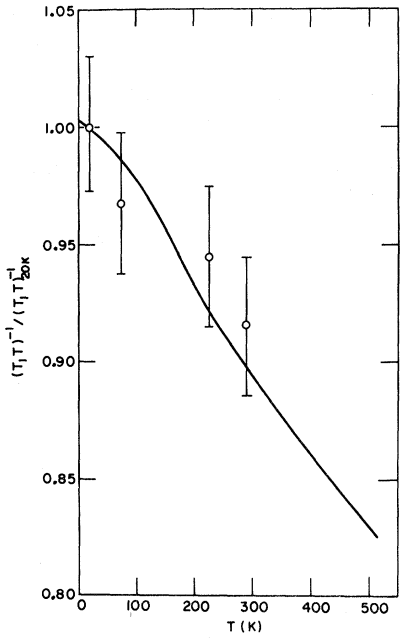

FIG. 6. Nuclear spin-lattice relaxation rate divided by the absolute temperature and normalized by the 20 K value. Circles denote the experimental values of Butterworth (Ref. 18) and the solid curve is the calculated value.

tribution to $(T_1T)^{-1}$ as

$$(T_1T)^{-1} = \kappa(\alpha,0)\,(T_1T)^{-1}_{\alpha=0}\; N(0)^{-2}\,[1-I\chi_0(T)]^{-2} \times \int f(\epsilon)\,[1-f(\epsilon)]\,N(\epsilon)^2\,d\epsilon \quad . \tag{4}$$

Taking the temperature-dependent core-polarization contribution to $(T_1T)^{-1}$ to be 50% of the total value of $(T_1T)^{-1}$ at 20 K, the variation of $(T_1T)^{-1}$ normalized by the 20-K value is shown in Fig. 6. There is good agreement with the experimental results. However, much better T_1T data are necessary over a wider temperature range in order to fully test the calculation. Because of the lack of exchange enhancement of the orbital contribution to T_1^{-1}, we have ignored the small temperature dependence of this term.

IV. CONCLUSION

In summary, we have found that the RAPW method as applied to Pt metal yields structure in the density of states arising from the 5th band that results in temperature dependences of the spin susceptibility, the electronic-specific-heat coefficient, the electrical resistivity, and the nuclear spin-lattice relaxation rate that are in good agreement with experiment above 20 K. Spin fluctuation contributions were not invoked. An essential element in the calculations is the high accuracy and resolution obtained by means of the analytic tetrahedron scheme as applied to the Fourier series representation of the RAPW bands. The results confirm the earlier work on Pd and lend greater confidence to the thermal calculations of the physical properties. We suggest that the calculation of the temperature dependence of the susceptibility, etc., is as severe a test of the band structure in the vicinity of E_F as in the calculation of the Fermi surface.

*Work supported by the U. S. Energy Research and Development Administration, the NSF, and the Air Force Office of Scientific Research.

[1]N. F. Berk and J. R. Schrieffer, Phys. Rev. Lett. 17, 433 (1966); S. Doniach and S. Englesberg, *ibid.* 17, 750 (1966).
[2]K. Andres and M. A. Jensen, Phys. Rev. 165, 533 (1968).
[3]P. F. de Chatel and E. P. Wohlfrath, Comments Solid State Phys. V, 133 (1973), and references therein.
[4]F. M. Mueller, A. J. Freeman, J. O. Dimmock, and A. M. Furdyna, Phys. Rev. B 1, 4617 (1970).
[5]O. K. Andersen and A. R. Mackintosh, Solid State Commun. 6, 285 (1968); O. K. Andersen, Phys. Rev. B 2, 883 (1970).
[6]F. Y. Fradin, Phys. Rev. Lett. 33, 158 (1974).
[7]J. E. van Dam and O. K. Andersen, Solid State Commun. 14, 645 (1974).
[8]J. B. Ketterson and L. R. Windmiller, Phys. Rev. Lett. 20, 321 (1968).
[9]J. B. Ketterson and L. R. Windmiller, Phys. Rev. B 2, 4814 (1970).
[10]J. C. Slater, Phys. Rev. 52, 198 (1937); T. L. Loucks, *ibid.* 139, 1333 (1965); *The Plane Wave Method* (Benjamin, New York, 1967).
[11]D. D. Koelling, A. J. Freeman, and F. M. Mueller, Phys. Rev. B 1, 1318 (1970); D. D. Koelling, Phys. Rev. 188, 1049 (1969).
[12]J. C. Slater, Phys. Rev. 81, 382 (1951).
[13]D. Liberman, J. T. Waber, and D. T. Cromer, Phys. Rev. 137, 27 (1965).
[14]G. Lehman and M. Taut, Phys. Status Solidi 54, 469 (1972); O. Jepsen and O. K. Anderson, Solid State Commun. 9, 1763 (1971).
[15]G. S. Knapp and R. W. Jones, Phys. Rev. B 6, 1761 (1972).
[16]A. M. Clogtson, V. Jacaarino, and Y. Yafet, Phys. Rev. B 4, A650 (1964).
[17]B. D. Budworth, F. E. Hoare, and J. Preston, Proc. R. Soc. Lond. A 257, 250 (1961).
[18]J. Butterworth, Phys. Rev. Lett. 8, 432 (1962).
[19]Y. Yafet and V. Jaccarino, Phys. Rev. 133, A6 (1964).
[20]A. Narath and H. T. Weaver, Phys. Rev. 175, 373 (1968).
[21]R. Jullien and B. Coqblin, J. Phys. (Paris) 35, I197 (1974).